Electronic and Nuclear Magnetic Relaxation in Crystals with Fluorite Structure Containing Eu^{2+} or Mn^{2+}†

JOSEPH B. HORAK* AND A. W. NOLLE
Department of Physics, The University of Texas, Austin, Texas
(Received 1 August 1966)

The spin-lattice relaxation time T_1 was measured for Eu^{2+} in BaF_2 and for Mn^{2+} in BaF_2 and SrF_2 at about 9 GHz. The nuclear relaxation time of the F^{19} nucleus was also measured at 29 MHz at temperatures below 77°K. Each impurity ion shows a one-phonon relaxation with $T_1 \propto T^{-1}$ in the liquid-helium region, and a Raman relaxation with $T_1 \propto T^{-5}$ at higher temperatures. In the Raman region, the matrix element of the dynamic crystalline field for Eu^{2+} in BaF_2 is smaller than for Eu^{2+} in CaF_2, in accordance with simple crystal-field theory. The opposite effect is observed for the case of the smaller Mn^{2+} ion; the matrix element decreases as the host lattice size decreases. A minimum in the T_1 vs T curve for the F^{19} nucleus occurs near 30°K for BaF_2 containing Mn^{2+} and near 50°K for SrF_2 containing Mn^{2+}, in approximate agreement with theory. For temperatures below the minima, the relaxation rate is attributed predominantly to the effect of Mn^{2+} pairs or clusters and to iron, which was found by spectroscopic analysis.

I. INTRODUCTION

FOR a given solid containing a paramagnetic impurity, a study of the temperature dependence of the spin-lattice relaxation T_1 of the impurity often makes it possible to distinguish between possible relaxation processes. Moreover, since a study of the temperature dependence of the nuclear spin-lattice relaxation time can yield information about the relaxation of the paramagnetic impurity and vice versa, it is advantageous to investigate magnetic relaxation of both kinds in the same series of samples.

Heitler and Teller,[1] Van Vleck,[2] Kronig[3] and others have shown that spin-lattice interaction of paramagnetic ions in solids can occur through the thermal modulation of the crystalline field. This theory predicts that a direct process predominates at low temperatures and that a Raman process (two-phonon) predominates at higher temperatures. For a spin system with an isolated doublet lying lowest in energy, this theory yields $T_1 \propto T^{-1}$ in the direct region and $T_1 \propto T^{-7}$ or $T_1 \propto T^{-9}$ in the Raman region. Orbach and Blume[4] predicted a T^{-5} dependence in the Raman region for a spin system having a multilevel state lowest in energy, in particular, Sm^{3+} in a field of cubic symmetry. In either case, the crystal field picture indicates that the relaxation time increases with increasing separation of the neighboring ions from the paramagnetic impurity.

In this paper we report the results of an investigation, primarily at low temperatures, of the paramagnetic relaxation times of Eu^{2+} in BaF_2 and Mn^{2+} in BaF_2 and SrF_2 and the nuclear relaxation time of the F^{19} nucleus in the BaF_2 and SrF_2 crystals doped with divalent manganese. The objectives of this investigation were fourfold: (1) To determine the mechanisms responsible for the relaxation of the paramagnetic impurities, where this can be done by paramagnetic resonance techniques; (2) to correlate the behavior of the relaxation of the paramagnetic impurities in BaF_2 and SrF_2 with the behavior reported for them in CaF_2 (a correlation in crystals having identical structures and differing only in their lattice spacing); (3) to identify the effects of the relaxation of Mn^{2+} impurities on the relaxation time of the F^{19} nucleus in single crystals of BaF_2 and SrF_2; (4) to determine as far as possible the other causes for the nuclear magnetic relaxation (NMR) of the F^{19} nucleus.

II. THEORY

A. Paramagnetic Relaxation Processes

We are interested in the relaxation processes of S-state ions. The crystalline field splitting for such ions is so small that any spin-orbit state (specified by **L** and **S**) can be considered as a multilevel state with splitting much less than kT.

In the direct process a phonon with energy equal to the Zeeman energy is absorbed (or, in the reverse process, emitted). In the direct process T_1 may be expressed approximately as[5]

$$\frac{1}{T_1}=\frac{3\delta^2 kT}{\pi\rho\hbar^4 V^5}|\langle a|\sum_{n,m} V_n{}^m|b\rangle|^2 \qquad (1)$$

for the case of a multilevel spin system, where δ is the resonant transition energy between spin states $|a\rangle$ and $|b\rangle$, ρ is the density of the crystal, V is the velocity of sound, and the $V_n{}^m$'s are components of the dynamic crystalline field. The sum of matrix elements shown between the vertical bars will be denoted by M_D.

The two-phonon or Raman process is one in which a phonon is absorbed and a virtual transition is effected from some initial state $|b\rangle$ to an excited state $|c\rangle$ at energy Δ_c, while another phonon is emitted and a

† Assisted by the National Science Foundation and by the U. S. Office of Naval Research.
* Present address: Texas Instruments, Inc., Dallas, Texas.
[1] W. Heitler and E. Teller, Proc. Roy. Soc. (London) **A155**, 629 (1936).
[2] J. H. Van Vleck, J. Chem. Phys. **7**, 72 (1939); Phys. Rev. **57**, 426 (1940).
[3] R. de L. Kronig, Physica **6**, 33 (1939).
[4] R. Orbach and M. Blume, Phys. Rev. Letters **8**, 478 (1962).
[5] R. Orbach, Proc. Roy. Soc. (London) **A264**, 458 (1961).

virtual transition is effected to the state $|a\rangle$, the energy difference between the phonons being the energy δ between states $|a\rangle$ and $|b\rangle$.

Orbach and Blume[4] have reported that for the case of a spin system having a multilevel ground state, and excited states only at relatively high energy, the Raman process operates through intermediate state(s) $|c\rangle$ within the multilevel state. In this case δ, $\Delta_c \ll kT$, with the result that T_1 may be approximately expressed as[6]

$$\frac{1}{T_1}=\frac{9\times 4!}{\pi^3\rho^2V^{10}\hbar^2}|\langle a|\sum_{n,m}V_n{}^m|c\rangle \times\langle c|\sum_{n',m'}V_{n'}{}^{m'}|b\rangle|^2\left(\frac{kT}{\hbar}\right)^5. \quad (2)$$

The quantity within the vertical bars will be denoted by $M_R{}^2$.

B. Nuclear Relaxation due to Paramagnetic Impurities

Spin relaxation of nuclei in a crystal containing paramagnetic impurities was first considered by Bloembergen[7] and then later by Khutsishvili[8] and de Gennes.[9] More recent detailed discussions have been presented by Blumberg[10] and Rorschach.[11]

There are two limiting cases of nuclear relaxation that need to be considered: (1) Diffusion limited, and (2) rapid diffusion. In the diffusion-limited case considered by Khutsishvili[8] and de Gennes,[9] the relaxation process is limited primarily by the rate of transfer of energy to the immediate neighborhood of an impurity ion by the spin-diffusion process. The nuclear T_1 is found to be expressed as

$$T_1=3/(8\pi ND\beta), \quad (3)$$

where N is the impurity concentration, D is the nuclear-spin diffusion coefficient, and $\beta=(C/D)^{1/4}$ is the pseudopotential radius introduced by de Gennes. C is the nuclear transition probability existing at a unit distance from the impurity ion and may be approximated after proper spatial averaging as

$$C=\frac{1}{5\pi}(\gamma_p\gamma_n\hbar)^2S(S+1)\frac{\rho}{1+(\nu\rho)^2}, \quad (4)$$

where γ_p and γ_n are the magnetogyric ratios of the paramagnetic ion and the nucleus, respectively; ρ is the impurity spin-lattice relaxation time (or the impurity spin-spin relaxation time, if this is shorter); ν is the nuclear Larmor frequency; S is the total spin of the paramagnetic impurity.

In the rapid diffusion case, the nuclear relaxation is limited by the relaxation rate near the impurity ion. Blumberg[10] considered this case and found

$$T_1=3b^3/4\pi NC, \quad (5)$$

where b is referred to as the "barrier radius" inside of which spin-spin diffusion does not take place. Rorschach[11] defined the barrier radius "b" at which diffusion stops as

$$b=(3\langle\mu_p\rangle/\mu_n)^{1/4}a, \quad (6)$$

where a is the spacing between nuclei and $\langle\mu_p\rangle$ is the average magnetic moment of the impurity that is effective in quenching diffusion. Rorschach[11] has shown that

$$\langle\mu_p\rangle=g\mu_0S\left[B_s^2(x)+\frac{dB_s(x)}{dx}\frac{2}{\pi}\tan^{-1}\frac{\rho}{T_2}\right]^{1/2},$$

where

$$B_s(x)=\frac{(2S+1)}{2S}\coth\frac{2S+1}{2S}x-\frac{1}{2S}\coth\frac{x}{2S}$$

and T_2 is the nuclear spin-spin relaxation time. Here x is expressed as $gS\mu_0(H/kT)$, where g is the gyromagnetic ratio, and μ_0 is the Bohr magneton.

The diffusion-limited and rapid-diffusion cases mentioned above correspond to $\delta\gg 1$ and $\delta\ll 1$, respectively, where $\delta=\beta^2/2b^2$. In the diffusion-limited case, a nuclear magnetization gradient develops and is a maximum at a distance from the ion of the order of de Gennes pseudopotential radius β. This gradient will develop if $\beta>b$.

It is of interest to note that when $\rho\nu=1$, C is a maximum, and one should get a minimum in the T_1 versus temperature curve provided that b^3 varies slowly in the neighborhood of the minimum. An examination of Eqs. (3), (4), and (5) shows that the dependence of $1/T_1$ on ρ is stronger in the rapid-diffusion than in the diffusion-limited region. Thus a change in the slope of a plot of T_1 vs T should occur at the position where the diffusion-limited relaxation gives way to rapid-diffusion.

III. EXPERIMENTAL PROCEDURES

The EPR spectrometer used in these experiments was a Strand labs instrument operated at about 9 GHz (X band), modified for autodyne operation in such a way that the power incident upon the sample could be changed without changing the bias power reaching the microwave crystals. Philco germanium rectifiers, type L4153, which give a nearly constant noise figure above a few kHz, were used. This eliminated the use of the more difficult superheterodyne method of detection usually employed at low power levels.

Relative values of the electronic relaxation time were measured by the progressive saturation method,

[6] This expression differs by a factor of 8 from Eq. (27) in Chao-Yuan Huang, Phys. Rev. **139**, A241 (1965).
[7] N. Bloembergen, Physica **25**, 368 (1949).
[8] R. G. Khutsishvili, Proc. Inst. Phys., Acad. Sci. Geo. (USSR) **4**, 3 (1956).
[9] P. G. de Gennes, J. Phys. Chem. Solids **7**, 345 (1958).
[10] W. E. Blumberg, Phys. Rev. **119**, 79 (1960).
[11] R. E. Rorschach, Physica **30**, 38 (1964).

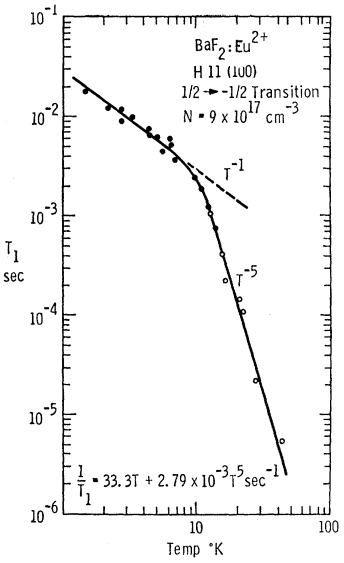

FIG. 1. Electronic relaxation data for Eu^{2+} in BaF_2. Filled circles, fast passage method. Open circles, saturation method (see text).

supplemented by absolute values obtained with a fast passage technique. The saturation data were analyzed by the method of Castner.[12] For relaxation times greater than 0.8 msec the fast passage technique was used.[13]

The nuclear T_1 was determined from the recovery of magnetization after the sample was saturated by a sufficiently rapid succession of 90° pulses. After a recovery time t, the magnetization $M_z(t)$ was indicated by the induced emf following another 90° pulse. A plot of $\ln[M_z(\infty)-M_z(t)]$ versus the waiting time t yields a straight line whose slope is T_1. For practical purposes, $M_z(\infty)$ is any value $M_z(t)$ obtained for $t>5T_1$.

All of the samples used in this study were either obtained commercially (Optovac Inc., North Brookfield, Massachusetts) or grown in the laboratory. For the samples grown in the laboratory we employed the Stockbarger[14] technique.

Some of the samples studied were annealed, with the expectation of reducing the clustering of impurities at dislocations. This involved heating the samples at about 900°C for 48 h and then cooling slowly over a period of about 6 h.

The concentrations were estimated from the EPR spectra and from analysis by optical spectroscopy.

IV. EXPERIMENTAL RESULTS AND DISCUSSION

A. Paramagnetic Relaxation

1. Eu^{2+} in BaF_2. The divalent europium ion belongs to the configuration $(4f)^7$ and has a ground state of $^8S_{7/2}$. The eightfold degeneracy of the ground state is partially lifted by a crystal field of cubic symmetry. The ground state is split, in the order of increasing energy, into a doublet Γ_7, a quartet Γ_8, and a doublet Γ_6.

The spectrum was first studied by Title,[15] and by Vinokurov *et al.*[16] At 9 GHz only the $\frac{1}{2}\rightarrow-\frac{1}{2}$ electronic transition is well resolved. To resolve the other transitions it is necessary to go to a higher frequency.

The spin-lattice relaxation time for the above transition with the magnetic field along the (100) direction is shown in Fig. 1. The outer hyperfine components for the transition were the ones studied. The data can best be fitted by

$$(1/T_1)=33.3T+2.79\times10^{-3}T^5\ \text{sec}^{-1}. \quad (7)$$

It is seen from observing the temperature dependence of the relaxation times that below about 11°K the single phonon process is dominant and that above this temperature the form of the two-phonon Raman process predicted by Orbach and Blume[4] is dominant.

The above observed temperature dependences agree with those reported for S-state ions in CaF_2. For Eu^{2+} in CaF_2 Huang[6] found that the relaxation time for the $\frac{1}{2}\rightarrow-\frac{1}{2}$ transition can best be fitted by

$$(1/T_1)=12T+5.3\times10^{-4}T^5\ \text{sec}^{-1}. \quad (8)$$

For Gd^{3+} ions in tetragonal sites in CaF_2, Bierig *et al.*[17] reported that T_1 for the $\frac{1}{2}\rightarrow-\frac{1}{2}$ transition may be expressed as

$$(1/T_1)=9.1\times10^2T^{1/2}+2.5\times10^{-4}T^5\ \text{sec}^{-1}. \quad (9)$$

The first term is not associated with the true spin-lattice relaxation time; Huang[6] has pointed out that there may have been cross relaxation with the neighboring transitions of Gd^{3+} ions present in trigonal sites in the samples used. Indeed Manekov and Pol'skii,[18] who studied Gd^{3+} in CaF_2 in the low-temperature region, reported a T^{-1} temperature dependence for Gd^{3+} in cubic sites and a weaker than T^{-1} dependence for Gd^{3+} in tetragonal and trigonal sites, in agreement with Bierig *et al.*[17]

Using an average sound velocity calculated from the experimental values of Gerlich[19,20] (as in Debye's specific heat theory) and comparing Eq. (2) with the second term in Eq. (7), we get an approximate value of 25 cm^{-1} for the matrix element of the dynamic crystalline field M_R.

Similarly, using an average velocity of sound for CaF_2 as calculated from the experimental values of Huffman and Norwood[21] and comparing Eq. (2) with

[12] T. G. Castner, Phys. Rev. **115**, 1058 (1959).
[13] J. B. Horak, doctoral dissertation, University of Texas, 1966 (unpublished).
[14] J. V. Stockbarger, J. Opt. Soc. Am. **39**, 731 (1949).
[15] R. S. Title, Phys. Letters **6**, 13 (1963).
[16] V. M. Vinokurov, M. M. Zaripov, V. G. Stepanov, G. K. Chirkin, and L. Ya. Shekum, Fiz. Tverd. Tela **5**, 1936 (1963) [English transl.: Soviet Phys.—Solid State **5**, 1415 (1964)].
[17] R. W. Bierig, M. J. Weber, and S. I. Warshaw, Phys. Rev. **134**, A1504 (1964).
[18] A. A. Manenkiv and Yu. E. Pol'skii, Zh. Eksperim. i Teor. Fiz. **45**, 1425 (1964) [English transl.: Soviet Phys.—JETP **18**, 985 (1964)].
[19] D. Gerlich, Phys. Rev. **135**, A1331 (1964).
[20] D. Gerlich, Phys. Rev. **136**, A1366 (1964).
[21] D. R. Huffman and M. H. Norwood, Phys. Rev. **117**, 709 (1960).

TABLE I. A summary of manganese-doped samples used in the electronic relaxation measurements.

Crystal	Source	Estimated manganese concentration (ions/cm³) Spectroscopic analysis	EPR spectrum
BaF_2 No. 1	Optovac	2×10^{19}	8.5×10^{17}
No. 2	Own lab	$>10^{19}$	2×10^{18}
No. 3	Own lab	5×10^{19}	6×10^{18}
SrF_2	Optovac	5×10^{18}	7×10^{17}

the second term of Eqs. (8) and (9), we obtain values for M_R of approximately 35 and 29 cm^{-1} for Eu^{2+}:CaF_2 and Gd^{3+}:CaF_2, respectively.

The relaxation data will now be related to the crystal field as given by the EPR spectra. Title[15] evaluated the parameter b_4, which is a measure of the fourth-order crystal field, from the spectra for Eu^{2+} in CaF_2, SrF_2, and BaF_2 and made a log-log plot of b_4 versus the nearest-neighbor distance. Figure 2 shows this plot as well as a plot of b_4 obtained for Gd^{3+} by Sierro.[22]

Let us consider that the relaxation is due to the modulation of the crystalline field and take b_4 to be an indication of the strength of this field. If we plot the log of the observed matrix elements for Eu^{2+} and Gd^{3+} in CaF_2 and Eu^{2+} in BaF_2 versus the log of the nearest neighbor distance, R, and adjust the y axis as in Fig. 2, we see that the ratios between these M_R values are nearly the same as the corresponding b_4 ratios. A value of about 22 cm^{-1} for the matrix element for Eu^{2+} in BaF_2 would best fit the curve. This is in reasonable agreement with our observed value of 25 cm^{-1} when one considers that the 10th power of an effective average sound velocity enters into the calculation of M_R.

In the direct relaxation region we find the following

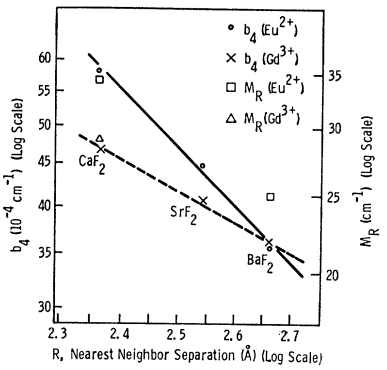

FIG. 2. Log-log plot of the Hamiltonian parameter b_4 versus the nearest-neighbor distance R. Dashed line: Sierro's results for b_4 versus R, for Gd^{3+}. Solid line: Title's results for b_4 versus R, for Eu^{2+}. The slope defined by the two M_R points (present work) is considered to be the same as that of Title's data. Further, the ratio of $M_R(Eu^{2+})$ to $M_R(Gd^{3+})$, both in CaF_2, is seen to be nearly the same as the ratio $b_4(Eu^{2+})$ to $b_4(Gd^{3+})$.

[22] J. Sierro, Phys. Letters 4, 178 (1963).

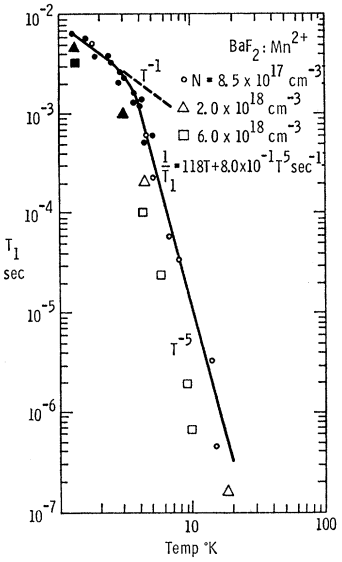

FIG. 3. Electronic relaxation data for different concentrations of Mn^{2+} in BaF_2. Sample No. 1, $N=8.5\times10^{17}/cm^3$; sample No. 2, $N=2\times10^{18}/cm^3$; sample No. 3, $N=6\times10^{18}/cm^3$. N represents the concentration of manganese ions giving an EPR spectrum. Filled symbols, fast passage method. Open symbols, saturation method (see text).

values for the matrix elements, M_D:

$$M_D=4.1\ cm^{-1} \quad \text{for} \quad BaF_2:Eu^{2+},$$
$$M_D=5.3\ cm^{-1} \quad \text{for} \quad CaF_2:Eu^{2+}.$$

An experimental value for Gd^{3+} in cubic sites is not available. However, we see that the ratio of the two values above agrees well with the corresponding ratio of M_R.

2. Mn^{2+} in BaF_2 and SrF_2. Mn^{2+} belongs to the $3d^5$ configuration and has a ground state of $^6S_{5/2}$. In a cubic field the ground state is split, in the order of increasing energy, into a twofold degenerate level Γ_7 and a fourfold degenerate level Γ_8, with a separation usually denoted by $3a$. In the present cases, $3a$ is sufficiently small that a transition can be identified by giving only the nuclear quantum number m, although the transition for a given m is actually a cluster of superhyperfine lines produced by interactions with F^{19} nuclei.

The spin-lattice relaxation times of manganese hyperfine transitions corresponding to $m=\frac{5}{2}$ and $m=-\frac{5}{2}$ are reported for a total of three BaF_2 and one SrF_2 crystals (see Table I). The results are shown in Figs. 3 and 4.

There was no apparent angular dependence for any of the crystals studied. Also, the relaxation times of the two hyperfine transitions were the same.

The curves in Figs. 3 and 4 can best be fitted by

$$\frac{1}{T}=118T+8.0\times10^{-1}T^5\ sec^{-1} \quad \text{for} \quad BaF_2:Mn^{2+} \quad (10)$$

and

$$\frac{1}{T}=154T+5.0\times10^{-2}T^5\ sec^{-1} \quad \text{for} \quad SrF_2:Mn^{2+}. \quad (11)$$

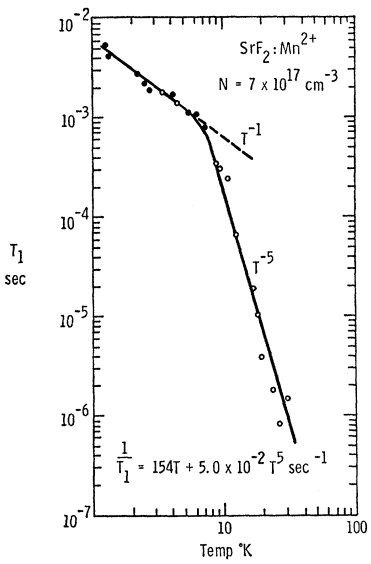

FIG. 4. Electronic relaxation data for Mn^{2+} in SrF_2. Filled circles, fast passage method. Open circles, saturation method (see text).

Here again we see a one-phonon process and the two-phonon process predicted by Orbach and Blume.[4]

If we follow the procedure we used in our analysis of Eu^{2+}, we get values for the matrix element of the dynamic crystalline field M_R of approximately 103 cm^{-1} and 79 cm^{-1} for Mn^{2+} in BaF_2 and SrF_2, respectively.

Using the relaxation data of Lay[23] for Mn^{2+} in CaF_2, we find $M_R=17$ cm^{-1}.

Thus we note a decrease in the value of M_R in the series BaF_2-SrF_2-CaF_2. This is just opposite to what simple crystal-field theory predicts. In seeking an explanation for this behavior, we notice that the Mn^{2+} ion when substituted in these crystals has a much greater size deficiency than Eu^{2+}, as may be seen from the ionic radius values 0.80, 1.12, and 1.35 Å for Mn^{2+}, Eu^{2+}, and Ba^{2+}, respectively. A severe size deficiency can make the center of the substitutional site an unstable position, as has been shown by dielectric[24,25] and anelastic[26] measurements for Li^+ or CN^- substituted in KCl. In the crystal-field picture of paramagnetic relaxation, this necessitates the inclusion in the orbit-lattice interaction of modulated second-order spherical harmonics, not included in the normal treatment for cubic lattices. Furthermore, the tunneling rate between stable positions can lie in the microwave frequency range,[25] and thus can contribute to the direct relaxation process at low temperatures.

In the direct region we find $M_D=7.7$ cm^{-1} for $BaF_2:Mn^{2+}$ and $M_D=13.4$ cm^{-1} for $SrF_2:Mn^{2+}$. Results of Lay[23] indicate a value of $M_D=7.9$ cm^{-1} for $CaF_2:Mn^{2+}$. We note that the values of M_D fail to show a monotonic change with lattice spacing. No attempt will be made to relate these to results in the Raman region, since the results in the direct region are particularly sensitive to cross relaxation with fast-relaxing impurities. An unidentified impurity was detected with the dc arc spectrometer in the SrF_2 sample. Iron in concentrations of 10^{17} to $10^{18}/cm^3$ was detected in all of the manganese-doped crystals we used.

TABLE II. A summary of manganese-doped samples used in the nuclear relaxation measurements.

Crystal	Source	Estimated manganese concentration (ions/cm^3) Spectroscopic analysis	EPR spectrum
BaF_2 No. 5	Own lab	$\geq 10^{19}$	2.7×10^{17}
No. 1	Optovac	2×10^{19}	8.5×10^{17}
SrF_2	Optovac	5×10^{18}	3×10^{17}

From Table I we see that the total concentration of manganese is greater than the concentration indicated by the intensity of the EPR spectrum. Pairs or clusters of manganese ions are therefore believed to exist. Pairs of manganese ions have been detected in MgO and ZnF_2 by paramagnetic resonance[27] and in ZnS from optical spectra.[28] There is the possibility of cross relaxation to such pairs.

The presence of paramagnetic species other than isolated Mn^{2+} ions is also indicated by our NMR results for low temperatures, in the next section.

B. Nuclear Relaxation

1. T_1 of F^{19} in $BaF_2:Mn^{2+}$. The two samples studied are described in Table II along with the SrF_2 sample. Here again we see that the total concentration of manganese in all kinds of sites is much greater than the concentration of manganese in sites giving a spectrum. Thus pairs or clusters of Mn^{2+} are believed to exist.

The data for the two BaF_2 samples are presented in Fig. 5. Our first concern is to verify the EPR relaxation measurements on Mn^{2+} from the NMR data.

The nuclear T_1 will have a minimum value (maximum C) when $\rho\nu=1$. Equation (10) indicates that ρ will satisfy this condition at about 28°K. A minimum is observed in both figures at about 30°K.

Using a value of $T_2=4.3\times10^{-5}$ sec, $b=1.4\times10^{-7}$ cm and $C=20.45\times10^{-40}$ cm^6/sec we find that $\delta=\beta^2/2b^2\sim1.7$ and consequently the diffusion-limited equation will apply. If we substitute the proper values for the quantities in Eq. (3) and if we use the experimentally observed values of T_1, we find approximately $N=6\times10^{16}/cm^3$ and $N=1\times10^{17}/cm^3$ for samples No. 5 and No. 1, respectively. We thus find order of magnitude agreement with the concentration estimated from the intensity of the EPR spectrum.

[23] F. Lay, doctoral dissertation, University of Texas, 1966 (unpublished).
[24] H. Bogardus and H. S. Sack, Bull. Am. Phys. Soc. 11, 229 (1966).
[25] A. I. Lakatos and H. S. Sack, Bull. Am. Phys. Soc. 11, 229 (1966).
[26] N. E. Byer, F. S. Welsh, and H. S. Sack, Bull. Am. Phys. Soc. 11, 229 (1966).
[27] J. Owen, J. Appl. Phys. 32, 213S (1961).
[28] D. S. McClure, J. Chem. Phys. 39, 2850 (1963).

Calculations of δ indicate that the rapid-diffusion equation should apply below 20°C. Since $\rho\nu \gg 1$, then the term C is inversely proportional to ρ. Consequently, from Eq. (5) we have

$$T_1 \propto \frac{b^3}{C} = T^{-5\frac{1}{2}}. \tag{12}$$

We note that our results differ considerably from this prediction. The relaxation below about 25° is evidently controlled by another impurity, the effect of which is also seen in the extreme shallowness of the minimum at 30°K.

In sample No. 5 we note a $T^{-3/4}$ temperature dependence. The presence of fast relaxing Mn-Mn pairs with relaxation times essentially independent of temperature could explain the observed results. In this case, C is independent of temperature and $T_1 \propto T^{-3/4}$.

For samples containing high concentrations of isolated impurity ions it is necessary to interpret the data by using the impurity spin-spin relaxation time in place of the electronic spin-lattice relaxation time. The spin-spin relaxation time T_2 is independent of temperature and Eq. (12) will again yield a $T^{-3/4}$ temperature dependence. However, our calculations show that this consideration is not important for the concentrations encountered in our crystals.

For sample No. 1 a minimum is observed in the vicinity of 10°K, and is tentatively attributed to iron satisfying the condition $\rho\nu = 1$. The amount of iron found to be present (10^{17} to 10^{18}/cm^3) is sufficient to account for the relaxation times observed. Iron was also detected in sample No. 5 where we do not observe a minimum in the vicinity of 10°K. This is not necessarily inconsistent; the concentration of iron encountered here is near the limit of the resolution of the dc arc spectrometer used in the spectroscopic analysis, and it is quite possible that the concentration of iron differs by a factor of 10 for the two samples.

A minimum attributed to Fe^{2+} has been reported in CaF_2 by Day *et al.*[29] in the vicinity of 20°K. A minimum at 14°K appears in the SrF_2 sample discussed in the next section and is also attributed to iron. In light of the behavior of ρ for Mn^{2+} in our crystals, a shift of the minimum attributed to iron to lower temperatures as we progress from CaF_2-SrF_2-BaF_2 might be expected.

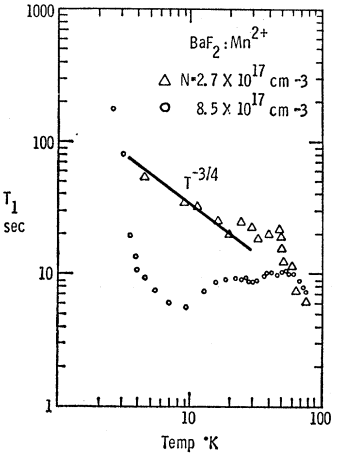

FIG. 5. Relaxation time of F^{19} nuclei in BaF_2. Sample No. 1, $N = 8.5\times10^{17}$/cm^3; sample No. 5, $N = 2.7\times10^{17}$/cm^3.

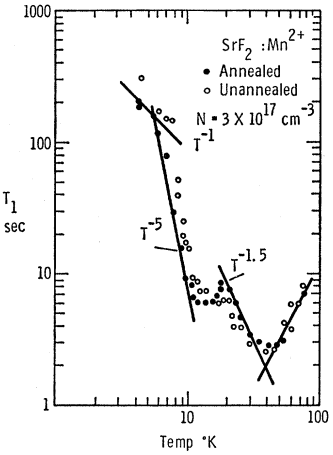

FIG. 6. Relaxation time of F^{19} nuclei in SrF_2 before and after annealing of the sample.

2. T_1 of F^{19} in SrF_2:Mn^{2+}. A sample of SrF_2 doped with divalent manganese was investigated before and after it was annealed as described in Sec. III. The results are shown in Fig. 6.

Again a minimum is expected when $\rho\nu = 1$, where ρ is the electronic spin lattice relaxation time and ν is the Larmor frequency. Equation (11) indicates that ρ will satisfy this condition at about 52°K and experimentally a minimum is observed near 50°K.

Using a value of 3.7×10^{-5} sec for the nuclear spin-spin relaxation time, 1.2×10^{-7} cm for the barrier radius, and 20.45×10^{-40} cm^6/sec for the term C, we find that $\delta = \beta^2/2b^2$ is approximately equal to 2.3. Therefore, diffusion-limited relaxation dominates. From Eq. (3) and the experimental value of T_1 we calculate a value of $N = 3.6\times10^{17}$/cm^3.

The EPR samples, for which concentration estimates could be easily made, generally showed an increase in the concentration of ions contributing to the EPR spectrum after being annealed. The SrF_2 sample used for the NMR measurements could not be examined before the annealing process without destroying its usefulness. (The large NMR sample would have to cut into smaller pieces for EPR work.) However, our NMR results in the vicinity of 50°K seem to indicate that the concentration was not increased.

The data for the unannealed sample show what appears to be a shoulder in the curve in the vicinity of 15°K. The apparent minimum is greatly enhanced after the sample is annealed. Spectroscopic analysis shows that iron is present in the crystals before and after annealing. Since the concentrations fall near the resolution limit of the dc arc spectrometer, it is not possible to determine from it whether the concentration

[29] S. M. Day, E. Otsuka, and B. Josephson, Jr., Phys. Rev. **137**, A108 (1965).

of iron has increased after the sample is annealed. Neither would a change of valence state be detectable. The fact that the sample was annealed in an iron bomb makes it possible that additional iron was diffused into the sample. If we assume that the minimum in the curve occurs for the condition $\rho\nu=1$, where ρ is the relaxation time of the iron impurity, then concentrations of iron of the magnitude observed in the sample, approximately 10^{17} ions/cm^3, could explain the relaxation times observed.

Below 14°K the temperature dependence of T_1 appears to reflect the transition from a Raman to a direct process for the paramagnetic ions, which cause the nuclear relaxation. However, we find that the observed nuclear T_1 is about 3 orders of magnitude too small to be explained as being due to isolated manganese ons, so that here again it is necessary to attribute the relaxation to other paramagnetic centers.

ACKNOWLEDGMENTS

We wish to thank R. G. Wittig for the construction of parts of the equipment used and W. B. Wollet for his assistance in solving many of the problems associated with vacuum systems and low temperatures. Special thanks is also due to B. Wardlaw of the Texas Department of Public Health for making a spectroscopic analysis of the crystals used in this work.

PHYSICAL REVIEW VOLUME 153, NUMBER 2 10 JANUARY 1967

Electric Field Shift in Electron Paramagnetic Resonance for Mn^{2+} in $CaWO_4$

A. KIEL AND W. B. MIMS
Bell Telephone Laboratories, New York, New York

(Received 13 June 1966)

The electric field shifts in paramagnetic resonance of Mn^{2+} in $CaWO_4$ have been measured and the components of the third-rank tensor defining the change in the spin Hamiltonian have been derived from the measurement. The theoretical determination of the tensor elements using an "equivalent even field" technique gave values at least a factor of 10 too small. Two possible mechanisms for the anomalously large shifts observed in Mn^{2+} are discussed, one based on the explicit mixture of odd states into the ground manifold, the other on ionic motion. The hypothesis that the first of these mechanisms is responsible for the large shifts implies that the normal D term of Mn^{2+} is $CaWO_4$ depends significantly on the strength of the odd crystal field.

THE effects of applied electric fields on the paramagnetic resonance of Ce^{3+}, Nd^{3+}, Er^{3+}, and Yb^{3+} ions in a $CaWO_4$ lattice have recently been investigated both experimentally[1] and theoretically.[2] In all these cases the ground state is an isolated Kramers doublet separated by >30 cm^{-1} from the next excited levels, and the electric effect can be adequately described in terms of modifications in the g values. Here we apply similar methods to the study of Mn^{2+}, an S-state ion, in which the changes in g can be neglected, and the electric effect manifests itself as a modification of the crystal-field splittings, i.e., in terms which are of the second order, and, to a lesser extent, of higher orders in the spin operators. As in the case of the rare-earth ions Mn^{2+} substitutes at the Ca^{2+} site, which has a point symmetry of $S_4(\bar{4})$, with the crystal c axis as the fourfold axis. There are two Mn sites, indistinguishable from one another in the absence of applied electric fields, which are related by the inversion operator. The Hamiltonian as given by Hempstead and Bowers[3] is

$$\begin{aligned}\mathcal{H}_0=&g_{\parallel}\beta H_z S_z+g_{\perp}\beta(H_x S_x+H_y S_y)+D(S_z^2-35/12)\\&+AS_zI_z+B(S_xI_x+S_yI_y)\\&+(a/6)(S_x^4-S_y^4+S_z^4-707/16)\\&+(7/36)F\{S_z^4-(95/14)S_z^2+81/16\},\end{aligned}\tag{1}$$

where

$$S=I=\tfrac{5}{2},\quad g_{\parallel}=1.99987,\quad g_{\perp}=1.99980,\quad D=-413\text{ Mc/sec},$$
$$a=13.8\text{ Mc/sec},\quad F=9.9\text{ Mc/sec},\quad A=-266.8\text{ Mc/sec},\quad B=-268.6\text{ Mc/sec}.$$

The z axis corresponds to the crystal c axis; the x and y axes in (1) are taken in the ab plane at an angle of 8° to the a and b axes. An applied electric field can, by reducing the symmetry of the environment, both modify or add terms to the Hamiltonian. We shall here consider primarily those terms which occur to the second power in the spin operators and which are linear in the applied electric field. In the general case these can be written as a contribution to the Hamiltonian

$$\mathcal{H}_E=E_iR_{ijk}S_jS_k,\tag{2}$$

[1] W. B. Mims, Phys. Rev. **140**, A531 (1965).
[2] A. Kiel, Phys. Rev. **148**, 247 (1966).
[3] C. F. Hempstead and K. D. Bowers, Phys. Rev. **118**, 131 (1960).